Environ Sci Pollut Res (2013) 20:399–412
DOI 10.1007/s11356-012-0855-7

RESEARCH ARTICLE

Removal of copper from water by electrocoagulation process—effect of alternating current (AC) and direct current (DC)

Ramakrishnan Kamaraj · Pandian Ganesan · Jothinathan Lakshmi · Subramanyan Vasudevan

Received: 8 February 2012 / Accepted: 5 March 2012 / Published online: 17 March 2012

Abstract
Purpose and aim In general, direct current (DC) is used in an electrocoagulation processes. In this case, an impermeable oxide layer may form on the cathode as well as corrosion formation on the anode due to oxidation. This prevents the effective current transfer between the anode and cathode, so the efficiency of electrocoagulation processes declines. These disadvantages of DC have been diminished by adopting alternating current (AC) in electrocoagulation processes. The main objective of this study is to investigate the effects of AC and DC on the removal of copper from water using magnesium alloy as anode and cathode.
Materials and methods Magnesium alloy of size 2.0 dm^2 was used as anode and as cathode. To optimize the maximum removal efficiency, different parameters like effect of initial concentration, effect of temperature, pH, and effect of current density were studied. Copper adsorbed magnesium hydroxide coagulant was characterized by SEM, EDAX, XRD, and FTIR.
Results The results showed that the optimum removal efficiency of copper is 97.8 and 97.2 % with an energy consumption of 0.634 and 0.996 kWh/m^3 at a current density of 0.025 A/dm^2, pH of 7.0 for AC and DC, respectively. The adsorption of copper is preferably fitting the Langmuir adsorption isotherm for both AC and DC respectively. The adsorption process follows the second-order kinetics model with good correlation. Temperature studies showed that adsorption was endothermic and spontaneous in nature.
Conclusions The magnesium hydroxide generated in the cell removes the copper present in the water, reducing the copper concentration to less than 1 mg/L, making it safe for drinking. The results of the scale-up study show that the process was technologically feasible.

Keywords Electrocoagulation · Alternating/direct current · Copper removal · Adsorption kinetics · Isotherms

1 Introduction

The presence of heavy metals in the aquatic environment is a source of great environmental alarm. Copper is known to be one of the most toxic heavy metals to living organisms and it is one of the more widespread heavy metal contaminants of the environment (Vinikour et al. 1980; James et al. 2006). Copper, a metal that occurs naturally in rocks, soil, water, and air throughout the environment, is an essential element in plants, animals, and humans (Billon et al. 2006). The adverse health effects caused by copper, mercury, and arsenic poisoning are far more catastrophic than any other natural calamity in the world in recent times (Ozer et al. 2004; Onmez and Aksu 1999; Prasad and Freitas 2000). The potential sources of copper in industrial effluents include metal cleaning and plating baths, pulp, paper board mills, wood pulp production, fertilizer industry, paints and pigments, municipal and storm water run-off, etc. (Boujelben et al. 2009). Common symptoms of copper toxicity are injury to red blood cells and lungs. It also gives damage to liver and pancreatic functions. Long-term exposure to copper may cause irritation to nose, mouth, and eyes; and also cause headaches, stomachaches, dizziness, vomiting, and diarrhea (Yu et al. 2000; Ajmal et al. 1998; Ozcan et al. 2005; Gardea-Torresde et al. 1996; Bailey et al. 1999). As

Responsible editor: Vinod Kumar Gupta

R. Kamaraj · P. Ganesan · J. Lakshmi · S. Vasudevan (✉)
CSIR—Central Electrochemical Research Institute,
Karaikudi 630 006, India
e-mail: vasudevan65@gmail.com

recommended by the World Health Organization, the drinking water guideline value is 2 mg/L. The United States Environmental Protection Agency (USEPA) has set the maximum contaminant level of copper allowed in drinking water is 1.3 mg/L (CPCB 2002). The conventional methods for removing copper from water include ion exchange, reverse osmosis, co-precipitation, coagulation, electrodialysis, and adsorption (Larous et al. 2005; Ozcan et al. 2005; Papandreou et al. 2007; Villaescesa et al. 2004; Saeed et al. 2005; Fiol et al. 2006; Shukla and Sakhardane 1992; Jain et al. 1997, 1995b; Jain et al. 1995a; Gupta et al. 2002; Gupta and Rastogi 2008a; Gupta et al. 2009a, b, c, d; Gupta and Rastogi 2010). The physical methods such as ion exchange, reverse osmosis and electrodialysis have proven to be either too expensive or inefficient to remove copper from water. Nowadays, the chemical treatment methods are not used due to heavy maintenance costs, problems pertaining to sludge handling and its disposal, and neutralization of the effluent.

Recent studies have demonstrated that electrocoagulation method offers an attractive alternative to the traditional methods for treating water (Vasudevan et al. 2008, 2009, 2010a, b, c, d, e; Vasudevan and Lakshmi 2011; Ali et al. 2011, 2012). In this process, anodic dissolution of metal electrode takes place with the evolution of hydrogen gas at the cathode. Electrochemically generated metallic ions from the anode can undergo hydrolysis to produce a series of activated intermediates that are able to adsorb, like chemical adsorption process (Gupta et al. 2006a, b, c, 1997a, b, 2003a, b, 2007a, b, c, d, e, f, 1998, 1999, 2001, 2002; Gupta 1998; Gupta and Sharma 2002; Gupta and Rastogi 2008a, b, 2009; Gupta and Ali 2000; Mittal et al. 2010; Mohan et al. 2001; Srivastava et al. 1995, 1996a, b, 1997; Ali and Gupta 2007; Ali 2010; Goyal et al. 2005, 2007a, b). The advantages of electrocoagulation are high particulate removal efficiency, compact treatment facility and the possibility of complete automation. This method is characterized by reduced sludge production, a minimum requirement of chemicals and ease of operation (Chen 2004; Adhoum and Monser 2004; Mrozowski and Zielinski 1983; Miwa et al. 2006; Onder et al. 2007; Carlesi Jara et al. 2007; Christensen et al. 2006; Carlos et al. 2006; Bailey et al. 1999). The overall reactions are as follows,

$$\text{At anode}: Mg^{2+}{}_{(aq)} + 2H_2O \rightarrow Mg(OH)_2 + 2H^{+}{}_{(aq)} \quad (1)$$

$$\text{At cathode}: 2H_2O_{(l)} + 2e^{-} \rightarrow H_{2(g)} + 2OH^{-} \quad (2)$$

Besides, the main disadvantage in case of aluminum electrode is the residual aluminum (The USEPA guidelines suggest maximum contamination is 0.05–0.2 mg/L) present in the treated water due to cathodic dissolution. This will lead to health problems like cancer. There is no such health problem in the case of magnesium electrode, because the USEPA guidelines suggest that the maximum contamination level of magnesium in water is 30 mg/L. Although there are numerous reports dealing with electrochemical coagulation as a means of removal of many pollutants from water and wastewater, there are few studies on copper removal by electrocoagulation method.

In general, direct current (DC) is used in an electrocoagulation processes. In this case, an impermeable oxide layer may form on the cathode as well as corrosion formation on the anode due to oxidation. These prevent the effective current transport between the anode and cathode, so the efficiency of electrocoagulation processes declines. These disadvantages of DC have been overcome by adopting alternating current (AC) in electrocoagulation processes. The main objective of this study is to investigate the effect of AC/DC on the removal efficiency of copper from water using magnesium as anode and cathode. To optimize the maximum removal efficiency of copper, the different parameters such as effect of initial concentration, effect of temperature, effect of current density, and pH were studied. In doing so, the equilibrium adsorption behavior is analyzed by fitting models of Langmuir, Freundlich, and Dubinin–Radushkevich (D–R) isotherms. Adsorption kinetics of electrocoagulants is analyzed using first-, second-order, Elovich, and Intraparticle kinetic models. The activation energy is evaluated to study the nature of adsorption.

2 Materials and methods

2.1 Experimental apparatus and procedures

The electrochemical cell (Fig. 1) consists of a 1.0 L glass vessel fitted with a PVC cover having suitable holes to introduce the electrodes, thermometer, pH sensor and electrolyte. Magnesium alloy (Magnesium Elektron Ltd; AZ31 consisting of 3.0 wt % Al, 1.0 wt % Zn) of size 2 dm^2 was used both as anode and cathode. The inter electrode gap between anode and cathode was 0.5 cm. The temperature of the electrolyte was controlled to the desired value with variation of ±2 K by adjusting the rate of flow of thermostatically controlled water through an external glass-cooling spiral. A regulated DC was supplied from a rectifier (10 Å, 0–25 V; Aplab model) and regulated AC was supplied from a source (0–5 A, 0–270 V, 50 Hz; AMETEK Model: EC1000S).

Copper nitrate ($CuNO_3$; Analar Reagent, Merck, Germany) was dissolved in de-ionized water for the required concentration. The pH of the electrolyte was adjusted, if required, with 1 M HCl or NaOH (Analar Reagent, Merck, Germany) solutions. Temperature studies were carried at varying temperatures (313–343 K) to determine the type of reaction. To examine the effect of co-existing ions, for the removal of

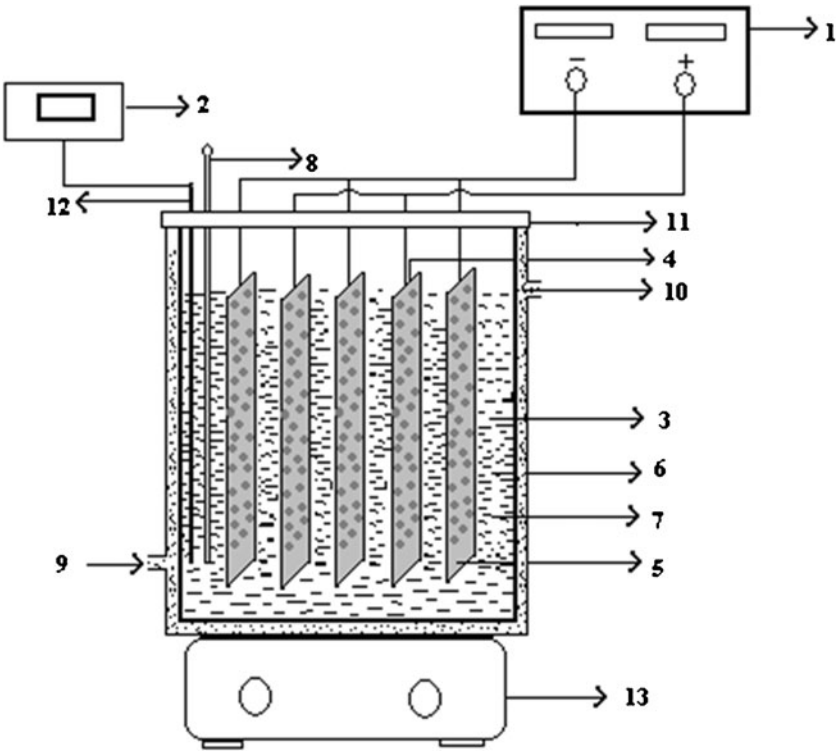

Fig. 1 Laboratory scale cell assembly. (*1*) DC Power Supply, (*2*) pH meter, (*3*) electrochemical cell, (*4*) cathodes, (*5*) anode, (*6*) electrolyte, (*7*) outer jacket, (*8*) thermostat, (*9*) inlet for thermostatic water, (*10*) outlet for thermostatic water, (*11*) PVC cover, (*12*) pH sensor and (*13*) magnetic stirrer

copper, Analar Grade (Merck, Germany) sodium salts of carbonate, phosphate, silicate, and fluoride were added to the electrolyte for required concentrations.

2.2 Analytical procedure

The copper was analyzed using UV–Visible Spectrophotometer (MERCK, Spectroquant Pharo 300, Germany) using MERCK kit. The SEM and EDAX of copper-adsorbed magnesium hydroxide coagulants were analyzed with a scanning electron microscope (SEM) made by Hitachi (model S-3000H). The XRD of electrocoagulation by-products were analyzed by a JEOL X-ray diffractometer (type—JEOL, Japan). The Fourier transform infrared spectrum of magnesium hydroxide was obtained using Nexus 670 FTIR spectrometer (Thermo Electron Corporation, USA). The concentration of carbonate, silicate, fluoride, and phosphate were determined using UV–Visible Spectrophotometer (MERCK, Pharo 300, Germany) with MERCK kit.

3 Results and discussion

3.1 Effect of pH

It has been established that the initial pH of the electrolyte is one of the important factor that affecting the performance of electrochemical processes particularly on the performance of electrocoagulation. To evaluate its effect, a series of experiments were performed, using 10 mg/L copper-containing solutions, with an initial pH varying in the range of 4–12 using the AC and DC source. From Fig. 2, it can be seen that the removal efficiency of copper was increased with increasing the pH and the maximum removal efficiency of 97.8 and 97.2 % was obtained at pH 7.0 for AC and DC, respectively. The percentage of copper removal increased with increasing pH 7, a decreasing trend in adsorption was

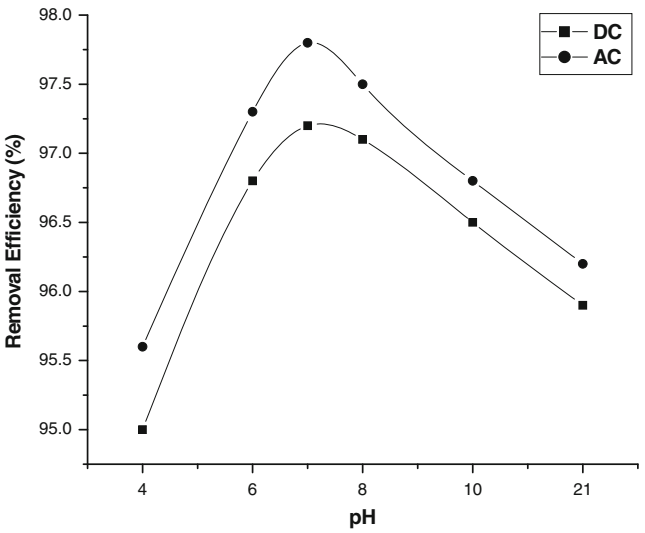

Fig. 2 Effect of pH on the removal of copper. Conditions—current density, 0.025 A/dm^2; concentration, 10 mg/L; and temperature, 303 K

observed when below and above pH 7 for both AC and DC source. At acidic and alkaline pHs, the oxide surfaces exhibit net positive and negative charges respectively and would tend to repulse the adsorption of copper and resulting the maximum adsorption at pH 7.0.

3.2 Effect of initial ion concentration

To study the effect of initial concentration, experiments were conducted at varying initial concentrations from 2 to 10 mg/L using AC and DC sources, and the results are illustrated in Fig. 3. From the results, it can be seen that the adsorption of copper is increased with an increase in copper concentration and it remains constant after equilibrium time. The equilibrium time was 10 min for all of the concentrations studied (2–10 mg/L) for the AC source. The amount of copper adsorption (q_e) increased from 1.77 to 8.92 mg/g when the concentration was increased from 2 to 10 mg/L for AC source. The figure also shows that the adsorption was rapid in the initial stages and gradually decreased with progress of adsorption. The plots are single, smooth and continuous curves leading to saturation, suggesting the possible monolayer coverage to copper on the surface of the adsorbent. In the case of DC the equilibrium time was found to be 45 min for all concentration studied (figure not shown).

3.3 Effect of current density

It is well known that the current density is the very important factor for elecrocoagulation process. The amount of copper removal and removal rate has increased by increasing current density. Further, the amount of copper removal depends upon the quantity of adsorbent (magnesium hydroxide) generated, which is related to the time and current density. To investigate the effect of current density on the copper removal, a series of experiments were carried out by solutions containing constant copper loading of 10 mg/L, at a pH 7.0, with current density being varied from 0.01 to 0.1 A/dm^2 using both AC and DC current source. The results showed that the optimum removal efficiency of 97.8 and 97.2 % with the energy consumption of 0.634 and 0.996 kWh/kL was achieved at a current density of 0.025 A/dm^2, at pH of 7.0 using AC and DC, respectively. The results are presented in Table 1. The results show that the removal efficiency of copper was higher and energy consumption was lower in the case of AC than DC. This may be due to the uniform dissolution of anode and cathode during electrocoagulation in the case of AC. The removal efficiency was found showing the amount of copper adsorption increases with the increase in adsorbent concentration, which indicates that the adsorption depends up on the availability of binding sites for copper. Hence, further studies were carried out at 0.025 A/dm^2

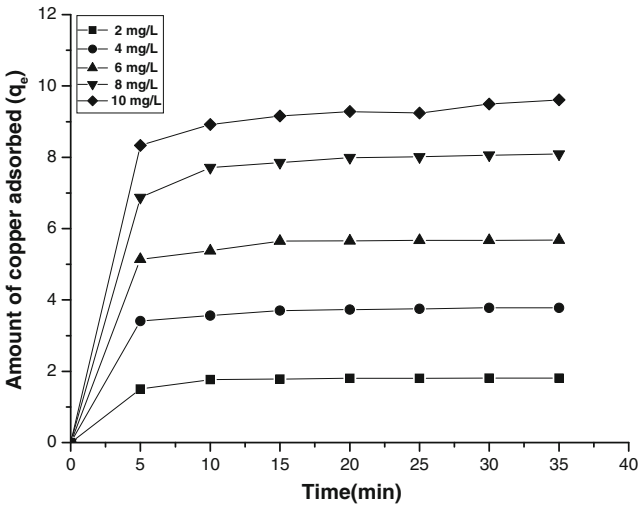

Fig. 3 Effect of electrolysis time and amount of copper adsorbed. Conditions—current density, 0.025 A/dm^2; pH, 7.0; and temperature, 303 K

3.4 Effect of co-existing ions

To study the effect of co-existing ions, in the removal of copper, sodium salts of carbonate (0–250 mg/L), phosphate (0–50 mg/L), silicate (0–15 mg/L), and arsenate (0 5.0 mg/L) was added to the electrolyte and electrolysis was carried out using AC.

The effect of carbonate on copper removal was evaluated by increasing the carbonate concentration from 0 to 250 mg/L in the electrolyte. The removal efficiencies are 97.8, 97, 79, 67.2, 33, and 24.5 % for the carbonate ion concentration of 0, 2, 5, 65, 150, and 250 mg/L respectively. From the results it is found that the removal efficiency of the copper is not affected by the presence of carbonate below 5 mg/L. A significant reduction in removal efficiency was observed, above

Table 1 Effect of current density on the removal efficiency of copper using AC and DC with initial copper concentration 10 mg/L

Current density (A/dm^2)	AC		DC	
	Removal efficiency (%)	Energy consumption (kWh/kL)	Removal efficiency (%)	Energy consumption (kWh/kL)
0.01	95.0	0.367	94.1	0.664
0.025	97.8	0.634	97.2	0.996
0.05	98.1	0.742	97.8	1.327
0.075	98.3	0.993	98.1	1.554
0.1	98.7	1.002	98.4	1.658

5 mg/L of carbonate concentration is due to the passivation of anode resulting, the hindering of the dissolution process of anode.

The concentration of phosphate ion was increased from 0 to 50 mg/L at the contaminant range of phosphate in the ground water. The removal efficiency for copper was 97.8, 96.9, 77.3, 55.1, and 50 % for 0, 2, 5, 25, and 50 mg/L of phosphate ion, respectively. There is no change in removal efficiency of copper below 5 mg/L of phosphate in the water. At higher concentrations (at and above 5 mg/L) of phosphate, the removal efficiency of copper decreased to 50 %. This is due to the preferential adsorption of phosphate rather than copper as the concentration of phosphate increase.

The effect of silicate on the removal efficiency of copper was investigated. The respective efficiencies for 0, 5, 10, and 15 mg/L of silicate are 97.8, 65, 60.2, and 53 %. The removal of copper decreased with increasing silicate concentration from 0 to 15 mg/L. In addition to preferential adsorption, silicate can interact with magnesium hydroxide to form soluble and highly dispersed colloids that are not removed by normal filtration.

From the results it is found that the efficiency decreased from 97.8, 88.1, 71.5, 52, and 26.7 % by increasing the concentration of fluoride from 0, 0.2, 0.5, 2, and 5 mg/L. This is due to the preferential adsorption of fluoride over copper as the concentration of fluoride increases. So, when fluoride ions are present in the water to be treated, fluoride ions compete greatly with copper ions for the binding sites.

3.5 Kinetic modeling

The dynamics of the adsorption process in terms of the order and the rate constant can be evaluated using the kinetic adsorption data. The process of copper removal from an aqueous phase by any adsorbent can be explained by using kinetic models.

3.5.1 First-order Lagergren model

The variation of the adsorbed copper with time was kinetically characterized using the First and second-order rate equation proposed by Lagergren. The first-order Lagergren model as (Wan Ngah and Hanafiah 2008; Ho and McKay 1998),

$$dq/dt = k_1(q_e - q_t) \quad (3)$$

where, q_t is the amount of copper adsorbed on the adsorbent at time t (in minutes) and k_1 (in per minute) is the rate constant of first-order adsorption. The integrated form of the above equation with the boundary conditions $t=0$ to $t>0$ ($q=0$ to $q>0$) and then rearranged to obtain the following time dependence function,

$$\log(q_e - q_t) = \log(q_e) - k_1 t/2.303 \quad (4)$$

where q_e is the amount of copper adsorbed at equilibrium. The q_e and rate constant k_1 were calculated from the slope of the plots of log ($q_e - q_t$) versus time (t).

3.5.2 Second-order Lagergren model

The second-order kinetic model is expressed as (Benaissa and Elouchd 2007; Wu et al. 2005),

$$dq/dt = k_2(q_e - q_t)^2 \quad (5)$$

Equation (5) can be rearranged and linearized as,

$$t/q_t = 1/k_2 q_e^2 + t/q_e \quad (6)$$

where q_e and q_t are the amount of copper adsorbed on Mg $(OH)_2$ (in milligrams per gram) at equilibrium and at time t (in minutes), respectively, and k_2 is the rate constant for the second-order kinetic model. The equilibrium adsorption capacity, q_e (in calories) and k_2 were determined from the slope and intercept of plot of t/q_t versus t (Fig. 4). Table 2 depicts the computed results obtained from first- and second-order kinetic model for AC and DC source. The calculated q_e values well agree with the experimental q_e values for second-order kinetics model better than the first-order kinetics model for both AC and DC. This implies that the second-order model is in good agreement with experimental data and can be used to favorably explain the copper adsorption on $Mg(OH)_2$.

3.5.3 Elovich model

The simplified form of Elovich model is (Oke et al. 2008),

$$q_t = 1/\beta \log_e(\alpha\beta) + 1/\beta \log_e(t) \quad (7)$$

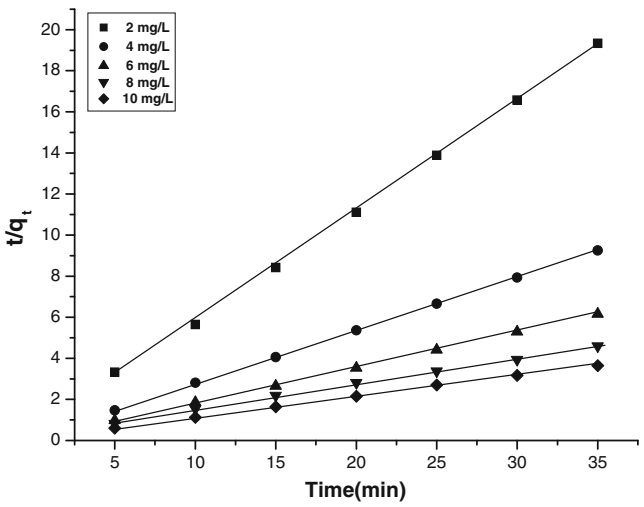

Fig. 4 Second-order kinetic model plot of different concentrations of copper. Conditions—current density, 0.025 A/dm^2; temperature, 303 K; and pH, 7.0

Table 2 Comparison between the experimental and calculated q_e values for different initial copper concentration in first- and second-order adsorption kinetics at room temperature

Current source	Concentration (mg/L)	q_e (exp)	First-order adsorption			Second-order adsorption		
			q_e (Cal)	$k_1 \times 10^3$ (min/mg)	R^2	q_e (Cal)	$k_2 \times 10^3$ (min/mg)	R^2
DC	2	1.79	1.454	−0.0556	0.8996	1.671	0.6655	0.9984
	4	3.61	3.253	−0.0124	0.9154	3.701	0.3361	0.9963
	6	5.44	5.112	−0.1102	0.8654	5.554	0.2995	0.9985
	8	6.67	6.454	−0.1243	0.8814	6.612	0.1559	0.9966
	10	9.01	8.221	−0.1332	0.8572	8.993	0.0999	0.9993
AC	2	1.77	1.5512	−0.0612	0.8431	1.7219	0.6789	0.9995
	4	3.56	3.1422	−0.0232	0.9629	3.6029	0.3591	0.9999
	6	5.38	5.0127	−0.1486	0.7818	5.4737	0.3005	0.9998
	8	6.51	6.2023	−0.0596	0.9334	6.5932	0.0541	0.9985
	10	8.92	8.0061	−0.0514	0.9428	8.2718	0.0971	0.9994

where α is the initial adsorption rate (in milligrams per gram per hour) and, β is the desorption constant (in grams per milligram). If copper adsorption fits the Elovich model, a plot of q_t versus $\log_e(t)$ should yield a linear relationship with the slope of $(1/\beta)$ and an intercept of $1/\beta \log_e (\alpha\ \beta)$. Table 3 depicts the results obtained from the Elovich equation. Lower regression value shows the inapplicability of this model.

3.5.4 Intraparticle diffusion model

Intraparticle diffusion is expressed as (Weber and Morris 1963; Allen et al. 1989),

$$R = k_{id}(t)^{\alpha z} \tag{8}$$

A linearized form of Eq. (8) is followed by

$$\log R = \log k_{id} + a \log(t) \tag{9}$$

in which a depicts the adsorption mechanism and k_{id} may be taken as the rate factor (percent of copper adsorbed per unit time). Lower and higher value of k_{id} illustrates an enhancement in the rate of adsorption and better adsorption with improved bonding.

Tables 2 and 3 depict the computed results obtained from first-order, second-order, Elovich, and Intraparticle diffusion models for AC and DC, respectively. The correlation coefficient values decreases from second-order, first-order, and Intraparticle diffusion to Elovich model. This indicates that the adsorption follows the second-order than the other models for both AC and DC. Further, the calculated q_e values well agrees with the experimental q_e values for second-order kinetics model concluding that the second-order kinetics equation is the best-fitting kinetic model.

3.6 Isotherm modeling

The adsorption capacity of the adsorbent has been tested using Freundlich, Langmuir and Dubinin–Redushkevich isotherms.

Table 3 Elovich model and Intraparticle diffusion for different initial copper concentrations at temperature 305 K and pH 7

Current source	Concentration (mg/L)	Elovich model			Intraparticle diffusion		
		A (mg/g/h)	B (g/mg)	1^2	k_{id} (l/h)	A (%/h)	R^2
DC	2	9.08	39.22	0.6941	30.11	0.225	0.6621
	4	4.63	31.45	0.8355	26.21	0.166	0.7026
	6	3.91	27.66	0.6665	20.36	0.092	0.7754
	8	1.09	20.31	0.7021	16.93	0.066	0.6452
	10	0.93	9.631	0.6654	15.22	0.056	0.5521
AC	2	10.13	51.42	0.7341	29.84	0.205	0.7143
	4	5.02	39.56	0.8434	25.46	0.188	0.6621
	6	3.43	24.33	0.6864	21.64	0.106	0.7045
	8	0.75	19.12	0.7146	18.02	0.091	0.8162
	10	0.41	10.24	0.6021	16.32	0.084	0.5561

Table 4 Constant parameters and correlation coefficient calculated for different adsorption isotherm models at different temperatures for copper adsorption on magnesium hydroxide

Isotherm	Constants				
Langmuir		q_m (mg/g)	b (L/mg)	R_L	R^2
	AC	277.12	0.0016	0.8894	0.9991
	DC	264.55	0.00125	0.9621	0.9999
Freundlich		k_f (mg/g)	n (L/mg)		R^2
	AC	0.9327	1.0166		0.9899
	DC	0.9025	1.0192		0.9876
D–R		Q_s			
	($\times 10^3$ mol/g)B	($\times 10^3$ mol^2/kJ^2)E (kJ/mol)			
	R^2AC0.9921.66410.210.9454DC1.8562.13412.360.9321				

These models have been widely used to describe the behavior of adsorbent–adsorbate couples. To determine the isotherms, the initial pH was kept at 7 and the concentration of copper used was in the range of 2–10 mg/L using AC and DC.

3.6.1 Freundlich isotherm

The Freundlich isotherm is an empirical model relates the adsorption intensity of the sorbent towards adsorbent. The isotherm is adopted to describe reversible adsorption and not restricted to monolayer formation. The mathematical expression of the Freundlich model can be written as (Leea et al. 2004; Prasanna Kumar et al. 2006),

$$q_e = KC^{n} \tag{10}$$

According to Freundlich isotherm model, initially amount of adsorbed compounds increases rapidly, this increase slow down with the increasing surface coverage. Equation (10) can be linearized in logarithmic form and the Freundlich constants can be determined as follows,

$$\log q_e = \log k_f + n \log C_e \tag{11}$$

where, k_f is the Freundlich constant related to adsorption capacity, n is the energy or intensity of adsorption; C_e is the equilibrium concentration of copper (in milligrams per liter). In testing the isotherm, the copper concentration used was 2–10 mg/L and at an initial pH 7, the adsorption data is plotted as logq_e versus logC_e and should result in a straight line with slope n and intercept k_f. The intercept and the slope are indicators of adsorption capacity and adsorption intensity, respectively. The value of n falling in the range of 1–10 indicates favorable sorption. The Freundlich constants k_f and n values were shown in Table 4 for AC and DC sources. From the analysis of the results, it is found that the Freundlich plots fit satisfactorily with the experimental data obtained in the present study.

Table 5 Pore diffusion coefficients for the adsorption of copper at various concentrations and temperature

	Pore diffusion constant $D \times 10^{-9}$ (cm^2/s)
Concentration (mg/L)	
2	1.112
4	1.006
6	0.965
8	0.883
10	0.767
Temperature (K)	
313	1.117
323	1.091
333	0.864
343	0.773

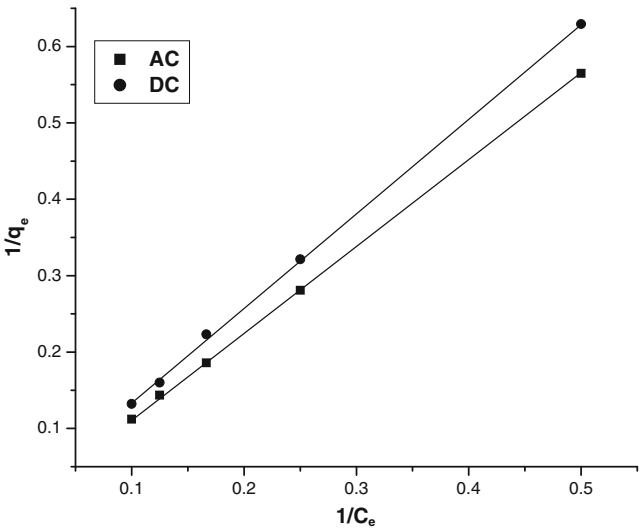

Fig. 5 Langmuir plot for adsorption of copper. Conditions—pH, 7.0; current density, 0.025 A/dm^2; and temperature, 303 K

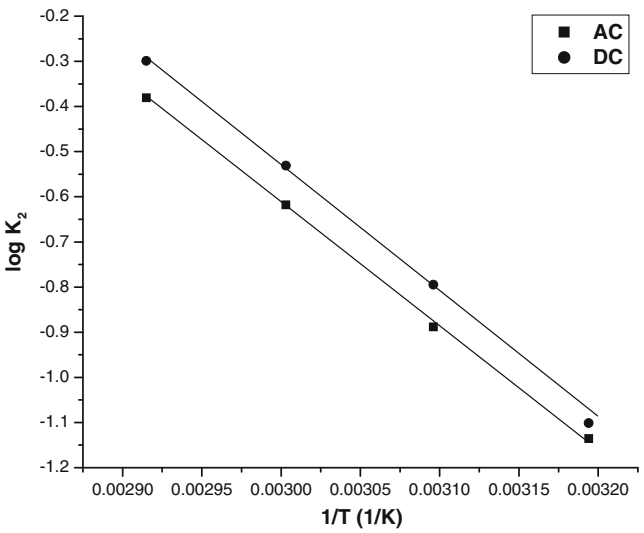

Fig. 6 Plot of log k_2 and 1/T. Conditions—pH, 7.0; current density, 0.025 A/dm^2

Table 6 Thermodynamic parameters for the adsorption of copper

Temperature (K)	AC				DC			
	K_c	ΔG^o (J/mol)	ΔH^o (kJ/mol)	ΔS^o (J/mol K)	K_c	ΔG^o (J/mol)	ΔH^o (kJ/mol)	ΔS^o (J/mol K)
313	0.2654	−711.33			0.2791	−726.03		
323	0.5411	−1333.15			0.5406	−1451.73		
			27.1165	0.0665			22.0181	0.07265
333	0.7654	−2566.1			0.7863	−2177.05		
343	1.1155	−2225.15			1.1738	−2903.03		

3.6.2 Langmuir isotherm

The linearized form of Langmuir adsorption isotherm model is (Bouzid et al. 2008; Sarioglu et al. 2005),

$$C_e/q_e = 1/q_m b + C_e/q_m \quad (12)$$

where, q_e is amount adsorbed at equilibrium concentration C_e, q_m is the Langmuir constant representing maximum monolayer adsorption capacity and b is the Langmuir constant related to energy of adsorption. The plots of $1/q_e$ as a function of $1/C_e$ for the adsorption of copper on $Mg(OH)_2$ are shown in Fig. 5. The plots were found linear with good correlation coefficients (>0.99) indicating the applicability of Langmuir model in the present study. The values of monolayer capacity (q_m) is found to be 277.21 and 264.55 mg/g for AC and DC (Table 4). The values of q_m calculated by the Langmuir isotherm were all close to experimental values at given experimental conditions. These facts suggest that copper is adsorbed in the form of monolayer coverage on the surface of the adsorbent.

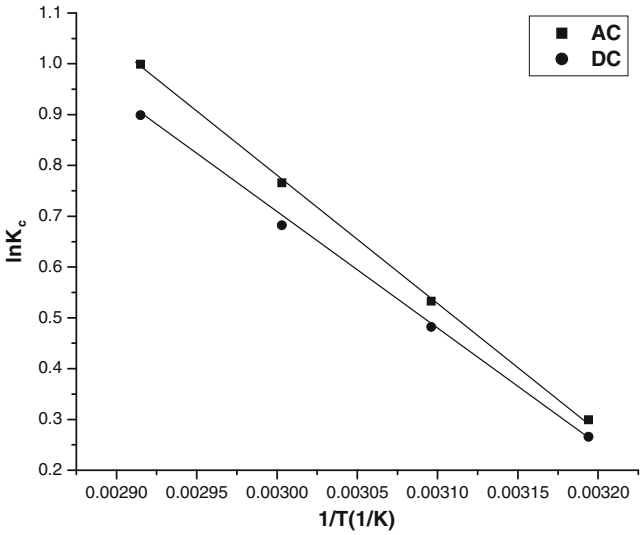

Fig. 7 Plot of log K_c and $1/T$. Conditions—pH, 7.0; current density, 0.025 A/dm^2

The essential characteristics of the Langmuir isotherm can be expressed as the dimensionless constant R_L.

$$R_L = 1/(1 + bc_o) \quad (13)$$

where R_L is the equilibrium constant it indicates the type of adsorption, b, is the Langmuir constant. c_o represents the various concentrations of copper solution. The R_L values between 0 and 1 indicate the favorable adsorption. The R_L values were found to be between 0 and 1 for all the concentration of copper studied.

3.6.3 Dubinin–Radushkevich isotherm

Dubinin and Radushkevich have proposed another isotherm which can be used to analyze the equilibrium data. It is not based on the assumption of homogeneous surface or constant adsorption potential, but it is applied to estimate the mean free energy of adsorption (E). This model is represented by (Tan et al. 2007),

$$q_e = q_s \exp\left(-B\varepsilon^2\right) \quad (14)$$

where $\varepsilon = RT \ln [1+1/C_e]$, B is related to the free energy of sorption per mole of the adsorbate as it migrates to the surface of the electrocoagulant from infinite distance in the solution and q_s is the D–R isotherm constant related to the degree of adsorbate adsorption by the adsorbent surface. The linearized form of Eq. (14):

$$\ln q_e = \ln q_s - 2BRT \ln[1 + 1/C_e] \quad (15)$$

The isotherm constants of q_s and B are obtained from the intercept and slope of the plot of $\ln q_e$ versus ε^2, respectively (Demiral et al. 2008). The constant B gives the mean free energy E, of adsorption per molecule of the adsorbate when it is transferred to the surface of the solid from infinity in the solution and the relation is given as,

$$E = [1/\sqrt{2B}] \quad (16)$$

The magnitude of E is useful for estimating the type of adsorption process. It was found to be 10.21 and 12.36 kJ/mol for AC and DC, respectively, which is bigger than the energy

Table 7 Comparison between the experimental and calculated q_e values for different initial copper concentrations of 10 mg/L in first and second-order adsorption kinetics at various temperatures and pH 7

Current source	Temperature (K)	q_e (exp)	First-order adsorption			Second-order adsorption		
			q_e (Cal)	k_1 (min/mg)	R^2	q_e (Cal)	k_2 (min/mg)	R^2
DC	313	7.61	1.601	−0.0061	0.8854	7.661	0.0762	0.9954
	323	8.86	2.112	−0.0054	0.8625	8.881	0.1561	0.9998
	333	9.11	3.122	−0.0046	0.8331	9.115	0.2552	0.9955
	343	9.21	4.077	−0.0039	0.7966	9.246	0.3656	0.9966
AC	313	7.35	1.563	−0.0026	0.9612	7.965	0.0731	0.9991
	323	8.81	2.012	−0.0018	0.6532	8.773	0.1626	0.9998
	333	9.08	3.001	−0.0011	0.8462	9.161	0.2513	0.9999
	343	9.16	4.165	−0.0063	0.7756	9.216	0.3432	0.9998

range of adsorption reaction, 8–16 kJ/mol. So the type of adsorption of copper on magnesium hydroxide was defined as chemical adsorption.

The correlation coefficient values of different isotherm models are listed in Table 4. The Langmuir isotherm model has a higher regression coefficient (R^2=0.999) when compared to the other models for both AC and DC source. The value of R_L for the Langmuir isotherm was calculated from 0 to 1, indicating the favorable adsorption of copper.

3.7 Thermodynamic parameters

The amount of copper adsorbed on the adsorbent increases by increasing the temperature indicating the process to be endothermic. The diffusion coefficient (D) for intraparticle transport of copper species into the adsorbent particles has been calculated at different temperature by,

$$t_{1/2} = 0.03x{r_o}^2/D \quad (17)$$

where $t_{1/2}$ is the time of half adsorption (s), r_o is the radius of the adsorbent particle (in centimeters), D is the diffusion coefficient in square centimeters per second. For all chemisorption systems, the diffusivity coefficient should be 10^{-5} to 10^{-13} cm^2/s (Yang and Al-Duri 2001). In the present work, D is found to be in the range of 10^{-10} cm^2/s. The pore diffusion coefficient (D) values for various temperatures and different initial concentrations of copper are presented in Table 5.

To find out the energy of activation for adsorption of copper, the second-order rate constant is expressed in Arrhenius form (Golder et al. 2006),

$$\ln k_2 = \ln k_o - E/RT \quad (18)$$

where k_o is the constant of the equation (in grams per milligram per minute), E is the energy of activation (in joules per mole), R is the gas constant (8.314 J/mol/K) and T is the temperature in kelvin. Figure 6 shows that the rate constants vary with temperature according to Eq. (18). The activation

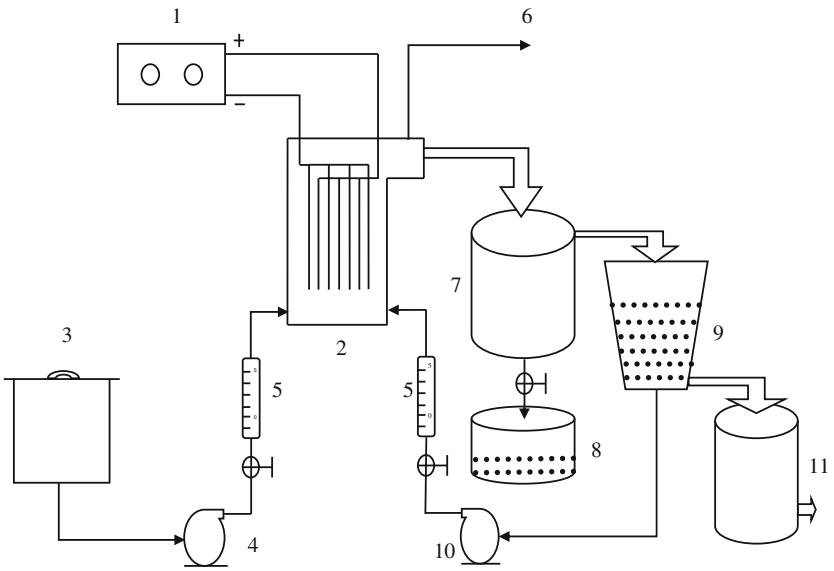

Fig. 8 Flow diagram of the pilot plant electrocoagulation system. (*1*) AC/DC Power Supply, (*2*) electro coagulation cell, (*3*) water tank, (*4*) inlet pump, (*5*) flow meter, (*6*) gas outlet, (*7*) setting tank, (*8*) sludge collection tank, (*9*) filtration unit, (*10*) recirculation pump, and (*11*) treated water

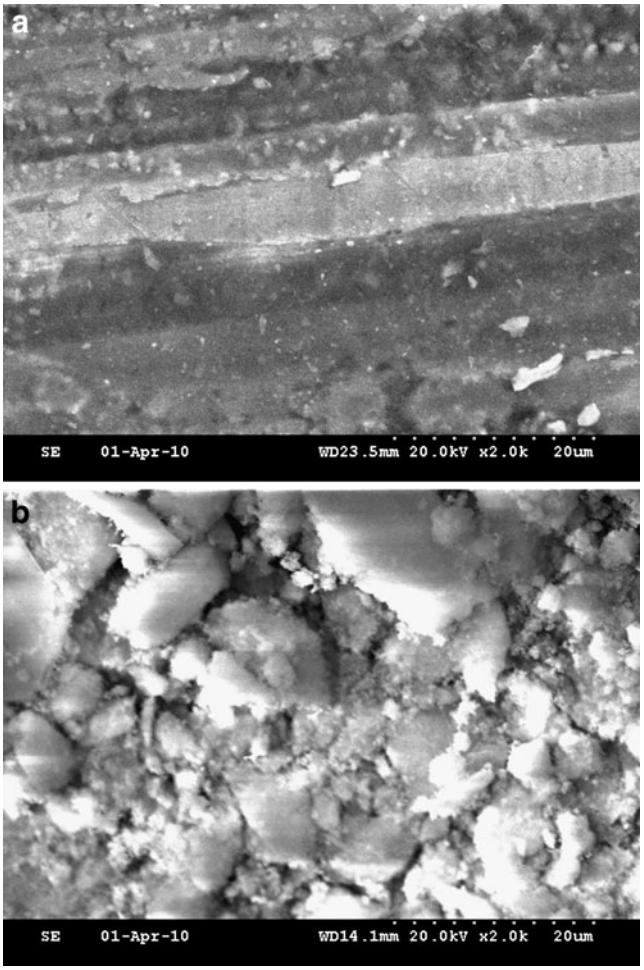

Fig. 9 SEM images of the anode after electrocoagulation by **a** AC and **b** DC

energy (0.445 and 0.336 kJ/mol for AC and DC, respectively) is calculated from slope of the fitted equation. The free energy change is obtained using the following relationship

$$\Delta G = -RT \ln K_c \tag{19}$$

where ΔG is the free energy (in kilojoules per mole), K_c is the equilibrium constant, R is the gas constant and T is the temperature in K. The K_c and ΔG values are presented in Table 6. From the table, it is found that the negative value of ΔG indicates the spontaneous nature of adsorption. Other thermodynamic parameters such as entropy change (ΔS) and enthalpy change (ΔH) were determined using the van't Hoff equation,

$$\ln K_c = \frac{\Delta S}{R} - \frac{\Delta H}{RT} \tag{20}$$

The enthalpy change and entropy change were obtained from the slope and intercept of the van't Hoff linear plots of $\ln K_c$ versus $1/T$ (Fig. 7). Positive value of enthalpy change (ΔH) indicates that the adsorption process is endothermic in nature, and the negative value of change in internal energy (ΔG) show the spontaneous adsorption of copper on the adsorbent. Positive values of entropy change show the increased randomness of the solution interface during the adsorption of copper on the adsorbent (Table 6). Enhancement of adsorption capacity of electrocoagulant (magnesium hydroxide) at higher temperatures may be attributed to the enlargement of pore size and or activation of the adsorbent surface (Vasudevan et al. 2010d). Using the Lagergren rate equation, first-order rate constants and correlation coefficients were calculated for different temperatures (305–343 K). The calculated q_e values obtained from the

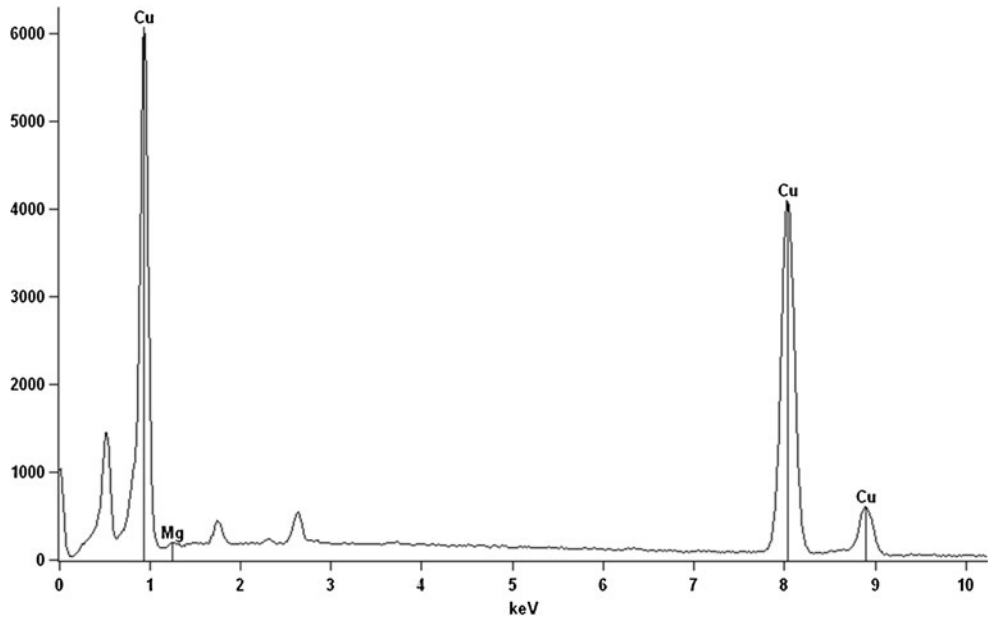

Fig. 10 EDAX for copper-adsorbed electrocoagulant

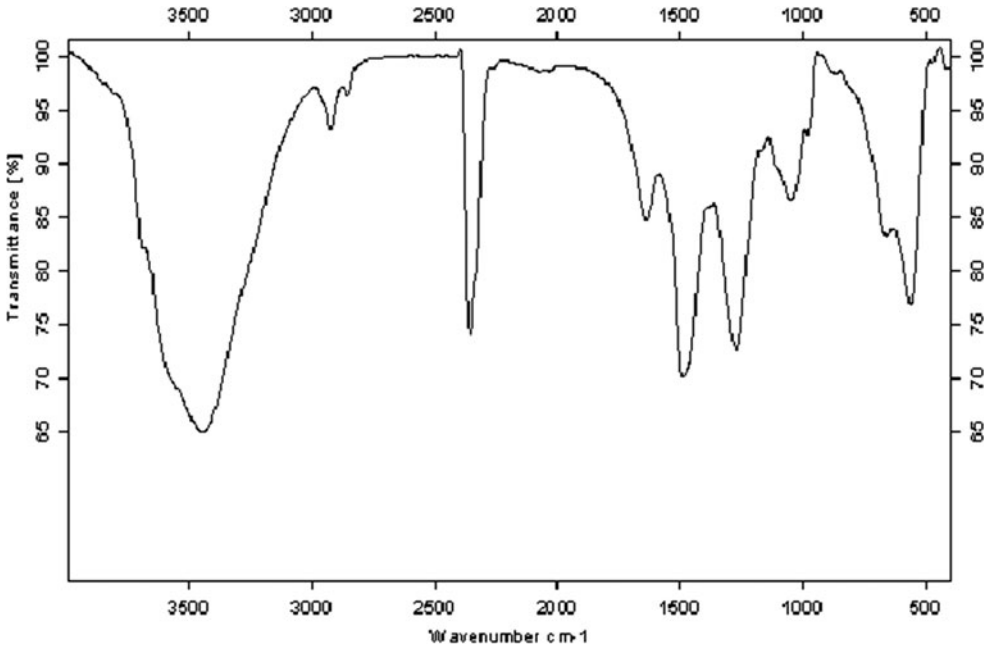

Fig. 11 FTIR spectrum of copper-adsorbed magnesium hydroxide

second-order kinetics agrees with the experimental q_e values better than the first-order kinetics model. Table 7 depicts the computed results obtained for the first- and second-order kinetic models using AC and DC. These results indicate that the adsorption follows second-order kinetic model at different temperatures used in this study.

3.8 Pilot scale study

A bench scale capacity cell (Fig. 8) was designed, fabricated and operated for the removal of copper from water. The system consists of AC/DC power supply, an electrochemical reactor, a water tank, a feed pump, a flow control valve, a flow measuring unit, a circulation pump, settling tank, sludge collection tank, filtration unit provisions for gas outlet and treated water outlet. The reactor is made of PVC with an active volume of 2,000 L. The magnesium anode and cathode each consist of five pieces situated approximately 5 mm apart from each other and submerged in the solution. The total electrode surface area is 1,500 cm^2 for both cathodes and anodes. The cell was operated at a current density of 0.025 A/dm^2 and the electrolyte pH of 7.0. The results showed that the removal efficiency of 97.8 and 97.2 % with the energy consumption of 0.634 and 0.996 kWh/kL was achieved at a current density of 0.025 A/dm^2 and pH of 7.0 using magnesium as electrodes using AC and DC, respectively. The results were consistent with the results obtained from the laboratory scale, showing that the process was technologically feasible.

3.9 Surface morphology

3.9.1 SEM and EDAX studies

In order to gain more insight into the effect of alternating current, the morphology of the electrode surface after two kinds of electrolysis (AC and DC) was characterized by SEM as shown in Fig. 9a and b. It can be observed that when the AC was fed, less disordered pores formed and a smooth microstructure of magnesium suggesting the magnesium electrodes were dissolved uniformly during the electrolysis. While for the electrodes fed with DC, the electrode surface is found to be rough, with a number of dents. These dents are formed around the nucleus of the active sites where the electrode dissolution results in the production of

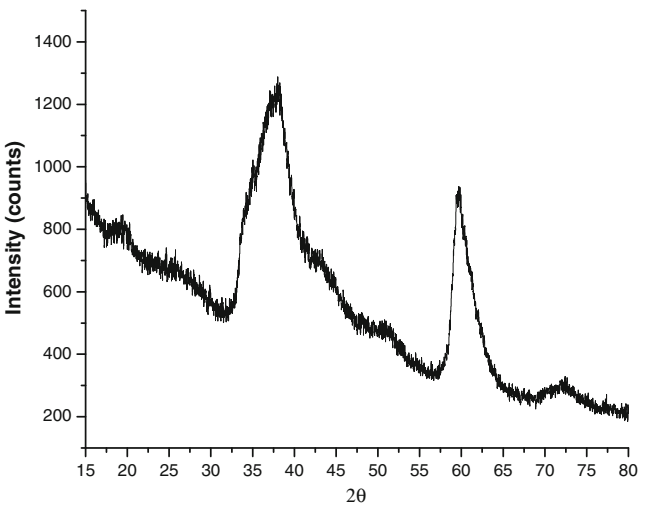

Fig. 12 XRD Spectra of Mg–Cu electrocoagulant

magnesium hydroxides. The formation of a large number of dents may be attributed to the anode material consumption at active sites due to the generation of oxygen at its surface (Li et al. 2009). Energy-dispersive analysis of X-rays was used to analyze the elemental constituents of copper-adsorbed magnesium hydroxide shown in Fig. 10. It shows that the presence of Cu, Mg, and O appears in the spectrum. EDAX analysis provides direct evidence that copper is adsorbed on magnesium hydroxide.

3.9.2 FTIR studies

FTIR spectrum (Fig. 11) of copper–magnesium hydroxide shows the sharp and strong peak at 3,452.84 cm^{-1} implies the transformation from free protons into a proton-conductive state in brucite. The 1,640.43 cm^{-1} peak indicates the bent vibration of H–O–H. The band at 669.93 cm^{-1} corresponds to Mg–O stretching vibration. Cu–O vibration at 875.21 cm^{-1} also observed.

3.9.3 XRD studies

X-ray diffraction spectrum of magnesium electrode coagulant showed very broad and sallow diffraction peaks (Fig. 12). This broad humps and low intensity indicate that the coagulant is amorphous or very poor crystalline in nature. This may be due to the crystallization of magnesium hydroxide is a very slow process resulting all magnesium hydroxides found to be either amorphous or very poorly crystalline.

4 Conclusion

The results showed that the optimized removal efficiency of 97.8 and 97.2 % was achieved for AC and DC source at a current density of 0.025 A/dm^2 and pH of 7.0 using magnesium as both anode and cathode. The magnesium hydroxide generated in the cell removes the copper present in the water, reducing the copper concentration to less than 1 mg/L, making it safe for drinking. The results of the scale-up study show that the process was technologically feasible. Langmuir adsorption isotherm was found to fit the equilibrium data for copper adsorption for both AC and DC. The adsorption process follows second-order kinetics. Temperature studies showed that adsorption was endothermic and spontaneous in nature.

Acknowledgment The authors wish to express their gratitude to the Director, Central Electrochemical Research Institute, Karaikudi, for aid in publishing this article.

References

Adhoum N, Monser L (2004) Decolourization and removal of phenolic compounds from olive mill wastewater by electrocoagulation. Chem Eng Process 43:1281–1287

Ajmal M, Khan A, Ahmad S, Ahmad A (1998) Role of sawdust in the removal of copper(II) from industrial wastes. Water Res 32:3085–3091

Ali I (2010) The quest for active carbon adsorbent substitutes: inexpensive adsorbents for toxic metal ions removal from wastewater. Sep Purf Rev 39:95–171

Ali I, Gupta VK (2007) Advances in water treatment by adsorption technology. Nat Protoc 1:2661–2667

Ali I, Khan TA, Asim M (2011) Removal of arsenic from water by electrocoagulation and electrodialysis techniques. Sepn Purfn Rev 40:25–42

Ali I, Khan TA, Asim M (2012) Removal of arsenate from ground water by electro-coagulation method. Environ Sci Polln Res. doi:10.1007/s11356-011-0681-3

Allen SJ, Mckay G, Khader KHY (1989) Intraparticle diffusion of basic dye during adsorption onto *Sphagnum* peat. Environ Pollut 56:39–50

Bailey SE, Olin TJ, Bricka RM, Adrian DD (1999) A review of potentially low-cost sorbents for heavy metals. Water Res 33:2469–2479

Benaissa H, Elouchd MA (2007) Removal of copper ions from aqueous solutions by dried sunflower leaves. Chem Eng Process 46:614–622

Billon L, Meric V, Castetbon A, Francois J, Desbrieres J (2006) Removal of copper ions from water of boilers by a modified natural based corncobs. J Appl Polym Sci 102:4637–4645

Boujelben N, Bouzid J, Elouear Z (2009) Adsorption of nickel and copper onto natural iron oxide-coated sand from aqueous solutions: study in single and binary systems. J Hazard Mater 163:376–382

Bouzid J, Elouear Z, Ksibi M, Feki M, Montiel A (2008) A study on removal characteristics of copper from aqueous solution by sewage sludge and pomace ashes. J Hazard Mater 152:838–845

Carlesi Jara C, Fino D, Specchia V, Saracco G, Spinelli P (2007) Electrochemical removal of antibiotics from wastewaters. Appl CatalsB: Environ 70:479–487

Carlos A, Huitle M, Ferro S (2006) Electrochemical oxidation of organic pollutants for the wastewater treatment: direct and indirect processes. Chem Soc Rev 35:1324–1340

Chen G (2004) Electrochemical technologies in wastewater treatment. Sep Purif Technol 38:11–41

Christensen PA, Egerton TA, Lin WF, Meynet P, Shaoa ZG, Wright NG (2006) A novel electrochemical device for the disinfection of fluids by OH radicals. Chem Commun 38:4022–4023

CPCB,Central Pollution Control Board (2002) Government of India, Delhi

Demiral H, Demiral I, Tumsek F, Karacbacakoglu B (2008) Adsorption of chromium (Vl) from aqueous solution by activated solution by activated carbon derived from olive bagasse and applicability of different adsorption models. Chem Eng J 144:188–195

Fiol N, Villaescesa I, Martinez M, Miralles N, Poch J, Serarols J (2006) Sorption of Pb(II), Ni(II), Cu(II) and Cd(II) from aqueous solutions by olive stone waste. Sep Purif Technol 50:132–140

Gardea-Torresde JL, Tang L, Salvador JM (1996) Copper adsorption by esterified and unesterified fractions of *Sphagnum* peat moss and its different humic substances. J Hazard Mater 48:191–206

Golder AK, Samantha AN, Ray S (2006) Removal of phosphate from aqueous solution using calcined metal hydroxides sludge waste generated from electrocoagulation. Sep Purif Technol 52:102–109

Goyal RN, Gupta VK, Sangal A, Bachheti N (2005) Voltammetric determination of uric acid at a fullerene-C60-modified glassy carbon electrode. Electroanalysis 17:2217–2223

Goyal RN, Gupta VK, Oyama M, Bachheti N (2007a) Gold nanoparticles modified indium tin oxide electrode for the simultaneous determination of dopamine and serotonin: application in pharmaceutical formulations and biological fluids. Talanta 72:976–983

Goyal RN, Gupta VK, Bachheti N (2007b) Voltammetric determination of adenosine and guanosine using fullerene-C60-modified glassy carbon electrode. Talanta 71:1110–1117

Gupta VK (1998) Equilibrium uptake, sorption dynamics, process development and column operations for the removal of copper and nickel from aqueous solution and wastewater using activated slag-a low cost adsorbent. Ind Eng Chem Res 37:192–202

Gupta VK, Ali I (2000) Utilization of bagasse fly ash (a sugar industry waste) for the removal of copper and zinc from wastewater. Sep Purif Technol 18:131–140

Gupta VK, Rastogi A (2008a) Biosorption of lead from aqueous solutions by green algae *Spirogyra* species: equilibrium and adsorption kinetics. J Hazard Mater 152:407–414

Gupta VK, Rastogi A (2008b) Equilibrium and kinetic modeling of cadmium (II) biosorption by nonliving algal biomass *Oedogonium* sp. from aqueous phase. J Hazard Mater 153:759–766

Gupta VK, Rastogi A (2009) Biosorption of hexavalent chromium by raw and acid-treated green alga *Oedogonium hatei* from aqueous solutions. J Hazard Mater 163:396–402

Gupta VK, Rastogi A (2010) Adsorption studies on the removal of hexavalent chromium from aqueous solution using a low cost fertilizer industry waste material. J Colloid Interface Sci 342:135–141

Gupta VK, Sharma S (2002) Removal of cadmium and zinc from aqueous solutions using red mud. Environ Sci Technol 36:3612–3617

Gupta VK, Ali I, Saini VK (1997a) Adsorption studies on the removal of Vertigo Blue 49 and Orange DNA13 from aqueous solutions using carbon slurry developed from a waste material. J Colloid Interface Sci 315:87–93

Gupta VK, Rastogi A, Dwivedi MK, Mohan D (1997b) Process development for the removal of zinc and cadmium from wastewater using slag—a blast furnace waste material. Sep Sci Technol 32:2883–2912

Gupta VK, Srivastava SK, Mohan D, Sharma S (1998) Design parameters for fixed bed reactors of activated carbon developed from fertilizer waste material for the removal of some heavy metal ions. Waste Manage 17:517–522

Gupta VK, Mohan D, Sharma S, Park KT (1999) Removal of chromium (VI) from electroplating industry wastewater using bagasse fly ash—a sugar industry waste material. Environmentalist 19:129–136

Gupta VK, Gupta M, Sharma S (2001) Process development for the removal of lead and chromium from aqueous solutions using red mud-an aluminum industry waste. Water Res 35:1125–1134

Gupta VK, Mangla R, Agarwal S (2002) Pb (II) selective potentiometric sensor based on 4-tert-Butylcalix [4] arene in PVC matrix. Electroanalysis 14:1127–1132

Gupta VK, Mohan D, Sharma S (2003a) Removal of lead from wastewater using bagasse fly ash—a sugar industry waste material. Sep Sci Technol 33:1331–1343

Gupta VK, Jain CK, Ali I, Sharma M, Saini VK (2003b) Removal of cadmium and nickel from wastewater using bagasse fly ash—a sugar industry waste. Water Res 37:4038–4044

Gupta VK, Mittal A, Gajbe V, Mittal J (2006a) Removal and recovery of the hazardous azo dye acid orange 7 through adsorption over waste materials: bottom ash and de-oiled soya. Ind Eng Chem Res 45:1446–1453

Gupta VK, Mittal A, Kurup L, Mittal J (2006b) Adsorption of a hazardous dye—erythrosine over hen feathers. J Colloid Interface Sci 304:52–57

Gupta VK, Jain AK, Kumar P, Agarwal S, Maheshwari G (2006c) Chromium(III)-selective sensor based on tri-*o*-thymotide in PVC matrix. Sens Actuat B: Chem 113:182–186

Gupta VK, Jain R, Mittal A, Mathur M, Shalini S (2007a) Photochemical degradation of the hazardous dye Safranin-T using TiO_2 catalyst. J Colloid Interface Sci 309:464–469

Gupta VK, Jain R, Varshney S (2007b) Removal of Reactofix golden yellow 3RFN from aqueous solution using wheat husk- an agricultural waste. J Hazard Mater 142:443–448

Gupta VK, Mittal A, Jain R, Mathur M, Sikarwar S (2007c) Photochemical degradation of hazardous dye—Safaranin-T Using TiO_2 Catalyst. J Colloid Interface Sci 309:460–465

Gupta VK, Singh AK, Gupta B (2007d) Schiff bases as cadmium (II) selective ionophores in polymeric membrane electrodes. Anal Chim Acta 583:340–348

Gupta VK, Jain R, Varshney S (2007e) Electrochemical removal of hazardous dye Reactofix Red 3 BFN from industrial effluents. J Colloid Interface Sci 312:292–296

Gupta VK, Ali I, Saini VK (2007f) Defluoridation of wastewaters using waste carbon slurry. Water Res 41:3307–3316

Gupta VK, Goyal RN, Sharma RA (2009a) Novel PVC membrane based alizarin sensor and its application; determination of vanadium, zirconium and molybdenum. Int J Electrochem Sci 4:156–172

Gupta VK, Al Khayat M, Singh AK, Pal MK (2009b) Nano level detection of Cd (II) using poly (vinyl chloride) based membranes of Schiff bases. Anal Chim Acta 634:36–43

Gupta VK, Goyal RN, Sharma RA (2009c) Comparative studies of neodymium (III)-selective PVC membrane sensors. Analytica Chim Acta 647:66–71

Gupta VK, Carrott PJM, Ribeiro Carrott MML (2009d) Low cost adsorbents: growing approach to wastewater treatment—a review. Critical Rev Environ Sci Technol 39:783–842

Ho YS, McKay G (1998) A comparison of chemisorption kinetic models applied to pollutant removal on various sorbents. Process Saf Environ Prot 76:332–340

Jain AK, Gupta VK, Singh LP (1995a) Neutral carrier and organic resin based membranes as sensors for uranyl ions. Anal Proc Anal Commun (RSC) 32:263–265

Jain AK, Gupta VK, Sahoo BB, Singh LP (1995b) Copper (II)-selective electrodes based on macrocyclic compounds. Anal Proc Anal Commun(RSC) 32:99–101

Jain AK, Gupta VK, Khurana U, Singh LP (1997) A new membrane sensor for UO^{2+}, based on 2-hydroxyacetophenoneoxime—thioureatrioxane resin. Electroanalysis 9:857–860

James R, Sampath K, Selvamani P (2006) Effect of ion-exchanging agent, zeolite on removal of copper in water and improvement of growth in *Oreochromis mossambicus* (Peters). Asian Fisheries Sci 13:317–325

Larous S, Meniai H, Bencheikh Lehocine M (2005) Experimental study of the removal of copper from aqueous solutions by adsorption using sawdust. Desalination 185:483–490

Leea C, Yanga W, Hsiehb C (2004) Removal of copper (II) by manganese-coated sandin a liquid fluidized-bed reactor. J Hazard Mater B114:45–51

Li X, Ma GB, Liu YY (2009) Synthesis and characterization of magnesium hydroxide using a bubbling setup. Ind Eng Chem Res 48:763–768

Mittal A, Jain R, Mittal J, Varshney S, Sirkarwar S (2010) Removal of Yellow ME 7 GL from industrial effluent using electrochemical and sorption technique. Int J Environ Pollution 43:308–323

Miwa DW, Malpass GRP, Machado SAS, Motheo AJ (2006) Electrochemical degradation of carbaryl on oxide electrodes. Water Res 40:281–289

Mohan D, Gupta VK, Srivastava SK, Chander S (2001) Kinetics of mercury adsorption from wastewater using activated carbon derived from fertilizer waste. Colloids and Surfaces A 177:169–181

Mrozowski J, Zielinski J (1983) Studies of zinc and lead removal from industrial wastes by electrocoagulation. Environ Prot Eng 9:77–85

Oke IA, Olarinoye NO, Adewusi SRA (2008) Adsorption kinetics for arsenic removal from aqueous solutions by untreated powdered eggshell. Adsorption 14:73–83

Onder E, Koparal AS, Ogutveren UB (2007) An alternative method for the removal of surfactants from water: electrochemical coagulation. Sep Purif Technol 52:527–532

Onmez G, Aksu Z (1999) The effect of copper(II) ions on the growth and bioaccumulation properties of some yeasts. Process Biochem 35:35–142

Ozcan A, Ozcan AS, Tunali S, Akar T, Kiran I (2005) Determination of the equilibrium, kinetic and thermodynamic parameters of adsorption of copper (II) ions onto seeds of *Capsicum annuum*. J Hazard Mater B124:200–208

Ozer A, Ozer D, Ozer A (2004) The adsorption of copper(II) ions onto dehydrated wheat bran (DWB): determination of the equilibrium and thermodynamic parameters. Process Biochem 39:2183–2191

Papandreou A, Stournaras CJ, Panias D (2007) Copper and cadmium adsorption on pellets made from fired coal fly ash. J Hazard Mater 148:538–547

Prasad MNV, Freitas H (2000) Removal of toxic metals from solution by leaf, stem and root phytomass of *Quercus ilex* L. (holly oak). Environ Pollut 110:277–283

Prasanna Kumar Y, King P, Prasad VSRK (2006) Removal of copper from aqueous solution using *Ulva fasciata* sp.—a marine green algae. J Hazard Mater B137:367–373

Saeed A, Iqbal M, Akhtar MW (2005) Removal and recovery of lead (II) from single and multimetal (Cd, Cu, Ni, Zn) solutions by crop milling waste (black gram husk). J Hazard Mater B117:65–73

Sarioglu M, May A, Cebeci Y (2005) Removal of copper from aqueous solutions by phosphate rock. Desalination 181:303–311

Shukla SP, Sakhardane VD (1992) Column studies on metal ion removal by dyed cellulosic materials. J Appl Poly Sci 44:903–910

Srivastava SK, Gupta VK, Dwivedi MK, Jain S (1995) Caesium PVC-Crown (dibenzo-24-crown-8) based membrane sensor. Anal Proc Anal Commun (RSC) 32:21–23

Srivastava SK, Gupta VK, Mohan D (1996a) Kinetic parameters for the removal of lead and chromium from wastewater using activated Carbon developed from fertilizer waste material. Environ Modell Assessment 1:281–290

Srivastava SK, Gupta VK, Jain S (1996b) A PVC-based benzo-15-crown-5 membrane sensor for cadmium. Electroanalysis 8:938–940

Srivastava SK, Gupta VK, Mohan D (1997) Removal of lead and chromium by activated slag—a blast-furnace waste. J Envorn Engg 123:461–468

Tan IAW, Hameed BH, Ahmed AL (2007) Equilibrium and kinetics studies on the basic dye adsorption by palm fibre activated carbon. Chem Eng J 127:111–119

Vasudevan S, Lakshmi J (2011) Effects of alternating and direct current in electrocoagulation process on the removal of cadmium from water. Sep Purifi Technol 80:643–651

Vasudevan S, Sozhan G, Ravichandran S, Jayaraj J, Lakshmi J, Margrat Sheela S (2008) Studies on the removal of phosphate from drinking water by electrocoagulation process. Ind Eng Chem Res 47:2018–2023

Vasudevan S, Lakshmi J, Sozhan G (2009) Studies on the removal of iron from drinking water by electrocoagulation—a clean process. Clean 37:45–51

Vasudevan S, Lakshmi J, Vanathi R (2010a) Electrochemical coagulation for chromium removal: process optimization, kinetics, isotherm and sludge characterization. Clean 38:9–16

Vasudevan S, Margrat Sheel S, Lakshmi J, Sozhan G (2010b) Optimization of the process parameters for the removal of boron from drinking water by electrocoagulation–a clean technology. J Chem Technol Biotech 85:926–933

Vasudevan S, Lakshmi J, Sozhan G (2010c) Studies relating to removal of arsenate by electrochemical coagulation optimization, kinetics, coagulant characterisation. Sep Sci Technol 45:1313–1325

Vasudevan S, Lakshmi J, Sozhan G (2010d) Studies on the removal of arsenate by electrochemical coagulation using aluminium alloy anode. Clean 38:506–515

Vasudevan S, Lakshmi J, Packiyam M (2010e) Electrocoagulation studies on removal of cadmium using magnesium electrode. J Appl Electrochem 40:2023–2032

Villaescesa I, Fiol N, Martinez M, Miralles N, Poch J, Serarols J (2004) Removal of copper and nickel ions from aqueous solutions by grape stalk wastes. Water Res 38:992–1002

Vinikour WS, Goldstein RM, Anderson RV (1980) Bioaccumulation patterns of zinc, copper, cadmium and lead in selected fish species from the Fox River, Illinois. Bull Environ Contam Toxicol 24:727–734

Wan Ngah WS, Hanafiah MAKM (2008) Adsorption of copper on rubber (*Hevea brasiliensis*) leaf powder: kinetic, equilibrium and thermodynamic studies. Biochemical En J 39:521–530

Weber WJ Jr, Morris JC (1963) Kinetics of adsorption on carbon from solutions. J SanitDiv Am Soc Civ Eng 89:31–59

Wu Z, Joo H, Lee K (2005) Kinetics and thermodynamics of the organic dye adsorption on the mesoporous hybrid xerogel. Chem Eng J 112:227–236

Yang XY, Al-Duri B (2001) Application of branched pore diffusion model in the adsorption of reactive dyes on activated carbon. Chem Eng J 83:15–23

Yu B, Zhang Y, Shukla A, Shukla SS, Dorris KL (2000) The removal of heavy metal from aqueous solutions by sawdust adsorption—removal of copper. J Hazard Mater 80:33–42